In Vivo Ablation of Plasmacytoid Dendritic Cells Inhibits Autoimmunity through Expansion of Myeloid-Derived Suppressor Cells

Marianna Ioannou,* Themis Alissafi,* Louis Boon,† Dimitrios Boumpas,*,‡ and Panayotis Verginis*

Autoimmunity ensues upon breakdown of tolerance mechanism and priming of self-reactive T cells. Plasmacytoid dendritic cells (pDCs) constitute a unique cell subset that participates in the activation of autoreactive T cells but also has been shown to be critically involved in the induction of self-tolerance. However, their functional importance during the priming phase of an organ-specific autoimmune response remains unclear. In this study, we demonstrate that absence of pDCs during myelin antigenic challenge resulted in amelioration of experimental autoimmune encephalomyelitis and reduced disease severity. This was accompanied by significantly decreased frequency of myelin-specific T cells in the draining lymph nodes and inhibition of Th1 and Th17 immune responses. Unexpectedly, in vivo ablation of pDCs increased myelopoiesis in the bone marrow and specifically induced the generation of $CD11b^{hi}Gr1^{+}$ myeloid-derived suppressor cells (MDSCs). Furthermore, we demonstrate that pDC depletion enhanced the mobilization of MDSCs in the spleen, and that sorted MDSCs could potently suppress $CD4^{+}$ T cell responses in vitro. Importantly, pDC-depleted mice showed increased levels of MCP-1 in the draining lymph nodes, and in vivo administration of MCP-1 increased the frequency and absolute numbers of MDSCs in the periphery of treated mice. Together, our results reveal that absence of pDCs during the priming of an autoimmune response leads to increased mobilization of MDSCs in the periphery in an MCP-1–dependent manner and subsequent amelioration of autoimmunity. ***The Journal of Immunology*****, 2013, 190: 2631–2640.**

Plasmacytoid dendritic cells (pDCs) constitute a unique subset of bone marrow (BM)–derived leukocytes that circulate in the blood in the steady-state and migrate to the lymph node (LN) under inflammatory conditions (1, 2). Functionally, pDCs possess a specialized ability to coordinate innate and adaptive immune responses under several pathological conditions (3). For example, virally infected pDCs secrete a large amount of type I IFN that contributes to antiviral defense, indicating an important role of this DC subset in innate immune responses (2). Furthermore, pDCs could uptake, process, and present Ags to T lymphocytes participating, therefore, in the initiation of an adaptive immune response (4–7). Finally, under certain conditions, pDCs have been shown to regulate aberrant immune responses in transplantation, asthma, and cancer mainly through induction of regulatory T cells (Tregs) (8–13), indicating a pivotal role of this cell subset in peripheral tolerance.

To date, increasing evidence implicates pDCs in the pathogenesis of systemic autoimmune diseases such as systemic lupus erythematosus and psoriasis (14–18). For example, infiltrating type I IFN-secreting pDCs have been demonstrated in the skin lesions of patients with systemic lupus erythematosus, where the severity and disease activity correlated with presence of type I IFN (18–20). In contrast, the role of pDCs in organ-specific autoimmune diseases remains controversial. First, in experimental autoimmune encephalomyelitis (EAE) and in a mouse model of rheumatoid arthritis, Ab-mediated depletion of pDCs during the acute phase significantly exacerbated the disease, indicating a regulatory role of pDCs during the progression of the autoimmune response (21, 22). In line with this, autoantigen presentation by pDCs inhibited EAE through induction of Tregs, and selective inhibition of MHC class II expression by pDCs exacerbated pathology (23). In contrast, depletion of pDCs during the priming of EAE significantly reduced disease onset and severity (24), suggesting a pathogenic role of this DC subset in the initiation of the autoimmune response. Overall, although pDCs have been shown to play a crucial role in the host defense mechanisms during viral infections, their precise role during the priming of an autoimmune response in vivo is not fully understood.

Myeloid-derived suppressor cells (MDSCs) are a heterogeneous population of cells that belong to the innate arm of the immune system and have been shown to exert immunosuppressive properties during cancer, inflammation, and infections (25). In mice, MDSCs are characterized by the coexpression of the myeloid-cell lineage differentiation Ag Gr-1 and CD11b, and can be further divided based on their morphology as monocytic or granulocytic MDSCs (26). Recently, we demonstrated a potent role of granulocytic MDSCs in suppressing autoimmune brain inflammation in mice and T cell responses in patients with multiple sclerosis

*Institute of Molecular Biology and Biotechnology, Foundation for Research and Technology, 71300 Heraklion, Greece; †Bioceros, BV 3584 CM Utrecht, The Netherlands; ‡Medical School, University of Crete, 71003 Iraklion, Crete, Greece

Received for publication July 9, 2012. Accepted for publication January 10, 2013.

This work was supported by grants from the Greek General Secretariat of Research and Technology (Synergasia to P.V.), European Union project Innovative Medicine Initiative 6 ("BTCure" to P.V. and D.B.), and a Bodossaki Foundation scholarship (to M.I.).

Address correspondence and reprint requests to Dr. Panayotis Verginis at the current address: Cellular Immunology and Immune Tolerance Laboratory, Division of Immunology and Transplatation, Foundation for Biomedical Research of the Academy of Athens, 4 Soranou Efessiou Street, 115 27 Athens, Greece. E-mail address: pverginis@bioacademy.gr

Abbreviations used in this article: 7AAD, 7-aminoactinomycin D; BM, bone marrow; cDC, conventional dendritic cell; dLN, draining lymph node; EAE, experimental autoimmune encephalomyelitis; LN, lymph node; MDSC, myeloid-derived suppressor cell; MOG, myelin oligodendrocyte glycoprotein; pDC, plasmacytoid dendritic cell; S.I., stimulation index; Treg, regulatory T cell.

in vitro (27). Specifically, MDSCs were significantly accumulated in the peripheral lymphoid compartments of mice with EAE, and they suppressed autoimmune responses in a PD-L1–dependent manner. However, the mechanism that is involved in the rapid accumulation and/or expansion of this suppressive cell population during the course of the autoimmune response remains unknown.

In this study, we sought to investigate the role of pDCs during the breakdown of self-tolerance in the EAE mouse model and delineate the mechanism through which pDCs are involved in the initiation of the autoimmune response. We demonstrate in this article that ablation of pDCs during the priming of EAE significantly reduced the clinical onset of disease and suppressed autoreactive T cell responses. Furthermore, pDC depletion was accompanied by increased myelopoiesis and mobilization of MDSCs in the peripheral lymphoid compartments that was driven by MCP-1.

Materials and Methods

Mice

Female C57BL/6 (B6) mice (6–10 wk old) were obtained from the specific pathogen-free facility of the Institute of Molecular Biology and Biotechnology (Heraklion Crete, Greece). Foxp3-GFP mice bred on B6 background were provided by Prof. A. Rudensky (Memorial Sloan-Kettering Cancer Center, New York, NY). CD11c-DTR/GFP mice were a kind gift of Prof. B. Lambrect (Ghent University, Belgium). All procedures were in accordance with institutional guidelines and were approved by the Greek Federal Veterinary Office.

In vivo depletion of pDCs and conventional DCs

Depletion of pDCs was achieved by injecting (i.p.) 400 μg 120G8 (IgG2a isotype) on days −1 and 1 (day 0: antigenic challenge) and 200 μg 120G8 on day 3. Efficient depletion was confirmed by FACS analysis of mPDCA-1 expression on homogenized draining LN (dLN) and spleen suspension. Depletion of conventional DCs (cDCs) was performed upon treatment of CD11cDTR mice with 50 ng/mouse diphtheria toxin (Sigma), injected i.p. at days −1 and 2 after myelin oligodendrocyte glycoprotein (MOG)/CFA immunization.

Reagents

For flow cytometric analysis, the following fluorescent-conjugated mAbs were used: anti–mPDCA-1 (JF05-1C2.4.1; Miltenyi Biotec); SiglecH (551) and CD45 (30-F11; both from BioLegend); Gr-1 (RB6-8C5), F4-80 (BM8), and NK1.1 (PK136; all from eBioscience); and CD11b (M1/70), CD3e (145-2C11), CD19 (1D3), CD45R/B220 (RA3-6B2), CD4 (RM4-5), CD8a (53-6.7), and CD11c (HL3; all from BD Pharmingen). OVA-Alexa Fluor 488 conjugate was obtained from Invitrogen and Molecular Probes. PE-conjugated $MOG_{38–49}/IA^b$ (MHC class II)–specific tetramer was obtained from the National Institutes of Heath tetramer facility.

Cell cultures were performed in DMEM, supplemented with 10% FBS, penicillin (100 U/ml) and streptomycin (100 μg/ml), and 2-ME (5×10^{-5} M; all from Life Technologies, Carlsbad, CA). $MOG_{35–55}$ peptide (MEVGWYRSPFSRVVHLYRNGK) was purchased from Genemed Biotechnologies.

EAE induction and histological assessment

EAE was induced in mice by immunization with 100 μg $MOG_{35–55}$ peptide emulsified in CFA (Sigma) s.c. at the base of the tail and i.p. injections of 200 ng pertussis toxin (Sigma) at the time of immunization and 48 h later. Mice were monitored daily for clinical signs of disease. Clinical scores of EAE were assessed as follows: 0, no disease; 1, limp tail; 2, hind-limb weakness; 3, hind-limb paralysis; 4, hind-limb and forelimb paralysis; 5, moribund state. Histological analysis of spinal cords from EAE mice were performed as described previously (27).

Flow cytometry and cell sorting

Cells were stained for extracellular markers for 20 min at 4°C in PBS/5% FBS. Dead cells were identified and excluded from all analyses by 7-aminoactinomycin D (7AAD; BD Pharmingen). For tetramer staining, LN cells (2×10^6 cells) were incubated for 5 min with 10% mouse and rat sera (Jackson Immunoresearch Laboratories) followed by 45-min staining with 10 μg/ml tetramer at room temperature. mAbs and viability dyes were added thereafter for 20 min on ice. Cells were acquired on a FACSCalibur (BD Biosciences) and analyzed using the FlowJo software (Tree Star). Cell sorting was performed using the high-speed cell sorter MoFlo (Dako).

T cell proliferation assays and cytokine assessment

Draining inguinal LNs were harvested 9–10 d after immunization and were cultured (6×10^5 cells/200 μl/well) at the presence or absence of $MOG_{35–55}$ peptide for 72 h. Cells were then pulsed with 1 μCi [^{3}H]thymidine (TRK120; Amersham Biosciences) for 18 h, and incorporated radioactivity was measured using a Beckman beta counter. Results are expressed as stimulation index (S.I.), which is defined as cpm in the presence of Ag/cpm in the absence of Ag. Cytokines were assessed in culture supernatants collected after 48 h of stimulation. Detection of IFN-γ (BD OptEIA; BD Biosciences) and IL-17 (R&D Systems) was performed by ELISA, following the manufacturer's recommendations.

In vitro suppression assays

Naive $CD4^+CD25^-$ T cells from the LNs of naive C57BL/6 mice were stained with CFSE (1 μM) in labeling buffer (PBS, 0.1% BSA for 10 min in 37°C) and either cultured alone or cocultured with sorted splenic $CD11b^{hi}$ $Gr1^+$ MDSCs at a ratio of 1:1 in the presence of plate-bound anti-CD3/anti-CD28 (10 and 1 μg/ml concentration, respectively). Proliferation of T cells was determined based on CFSE dilution by flow cytometry.

Detection of chemokines in LN homogenates

LNs were collected at day 4 after immunization and homogenized in homogenization buffer (PBS with Protease Inhibitor mixture-Roche) by using a glass homogenizer. Supernatants were collected by centrifugation, and chemokine levels were assessed by ELISA (mouse MCP-1 ELISA kit [eBioscience], mCCL19/CCL21 ELISA kit [R&D Systems]).

In vivo Ag uptake and BrdU incorporation

Alexa Fluor 488–conjugated OVA (100 μg/mouse) emulsified in CFA (1:1) was injected s.c. in C57/BL6 mice. Nine days after immunization, draining LN (dLN) cells were stained for specific markers and Ag uptake was measured using flow cytometric analysis. MOG/CFA immunized mice were i.p. administered with 1.5 mg BrdU/mouse at day 4 after immunization. Four hours after BrdU injection, spleens were harvested and analyzed by flow cytometry for BrdU incorporation, by using a BrdU flow kit (BD Pharmingen) according to the manufacturer's instructions.

Administration of rMCP-1 and rIFN-β

MOG/CFA immunized mice were injected i.p. with 1000 ng/mouse rMCP-1 (Peprotech) at days 3 and 4 after immunization; 4 h after the last injection, peripheral blood and spleens were analyzed for the frequency of $CD11b^{hi}$ $Gr1^+$ MDSCs by flow cytometry. In other experiments, MOG/CFA immunized mice were treated daily with 1 μg/mouse IFN-β1a (Rebif-Serono) from days 0–5. At day 6, spleens were dissected and analyzed by flow cytometry for the frequency of $CD11b^{hi}$ $Gr1^+$ MDSCs.

Enzymatic digestion of LNs for stromal cell isolation

Inguinal LNs from individual mice were dissected and placed in 2 ml freshly made enzyme mix composed of RPMI 1640 containing 0.1 mg/ml Dispase (Roche), 0.2 mg/ml collagenase P (Roche), and 0.1 mg/ml DNase I (Invitrogen). Tubes were incubated at 37°C in a waterbath for 30 min and mixed using a 1-ml pipette every 5 min until, when held up to light, it was clear that all remaining LN fragments were completely digested. Cells were filtered through 80-μm nylon mesh, washed, and resuspended in FACS buffer (5% FCS in PBS) for cell sorting.

RNA extraction and semiquantitative RT-PCR

RNA extraction and DNase I treatment were carried out with the RNeasy mini kit (Qiagen, Hilden, Germany), according to the manufacturer's instructions. RNA obtained from samples was reverse transcribed by using the Thermoscript RT-PCR system (Invitrogen). cDNA products were amplified by using Platinum Taq (Invitrogen) under the following conditions: a first step of 5 min at 94°C, followed for 40 s at 94°C, 40 s at 55°C, and 1 min at 72°C for 35 cycles. The conditions were chosen so that none of the cDNAs analyzed reached a plateau at the end of the amplification protocol. The primers used for MCP-1 (forward, 5′-TTAAAAACCTGGATCGGAACCAA-3′; reverse, 5′-GCATTAGCTTCAGATTTACGGGT-3′) and GAPDH (forward, 5′-CCAGTATGACTCCACTCACG-3′; reverse, 5′-CTCCTGGAAGATGGTGATGG-3′) yielded an amplification product of 121 and 98 bp, respectively. The PCR products were loaded onto ethidium bromide–stained, 2% agarose gels in Tris borate EDTA, and quantification of the band intensity was performed by ImageJ.

Statistics

The p values were derived using two-tailed Student t tests. All analyses were performed using Prism (GraphPad Software).

Results

Efficient and specific depletion of pDCs upon in vivo administration of 120G8 mAb

The role of pDCs during the breakdown of self-tolerance and the priming of the autoimmune response was investigated in the EAE mouse model, upon selective elimination of pDCs in vivo. Specifically, mice were treated with 120G8 mAb 1 d before and 2 d after antigenic challenge (day 0), as shown in Fig. 1A. Injection of 120G8 mAb efficiently depleted pDCs (gates were set on $7AAD^-CD3^-CD19^-CD11b^-$) in spleen and LNs as compared with untreated mice (Fig. 1B). The depletion efficiency in the organs was tested, reached 95%, and persisted for 2–3 d after the last injection. Because the 120G8 mAb recognizes the same epitope with the PDCA-1 mAb, we assessed the efficiency of pDC depletion in our system by using the SiglecH mAb that specifically expressed on murine pDCs (28). Flow cytometry analysis of dLNs revealed a distinct population of $CD11c^+SiglecH^+$ cells (gates were set in total $CD11c^+$ cells) in MOG/CFA-immunized animals that was almost absent in pDC-depleted, MOG/CFA-immunized animals (Fig. 1C). This finding indicates that administration of 120G8 mAb specifically eliminates pDCs in our system. Because a proportion of pDCs has been reported to express CD19 (29), we asked whether in vivo administration of 120G8 mAb differentially depletes CD19-expressing pDCs. To this end, we analyzed the LNs from pDC-depleted and control immunized mice for the expression of $SiglecH^+PDCA1^+CD19^+$ pDCs. As shown in Fig. 1D, both $SiglecH^+PDCA1^+CD19^+$ and $SiglecH^+PDCA1^+CD19^-$ pDCs are proportionally depleted in 120G8-treated animals (gates of $SiglecH^+PDCA1^+$ were set on whole LNs). Similar results were obtained in spleen (data not shown).

It was previously reported that the 120G8 mAb specifically depletes pDCs in naive mice, whereas under inflammatory situations, it could deplete a variety of immune cells (30, 31). We sought, therefore, to assess how administration of 120G8 in an autoimmune setting affected other cell types in the LNs, spleen, and BM. Of note, we did not observe any significant differences in the proportion of $NK1.1^+$ NK cells and $NK1.1^+CD3^+$ NKT cells (Fig. 1E, gates were set in total cells), $CD19^+B220^+$ B cells (Fig. 1F, gates were set on $CD3^-CD11b^-$ cell populations), and

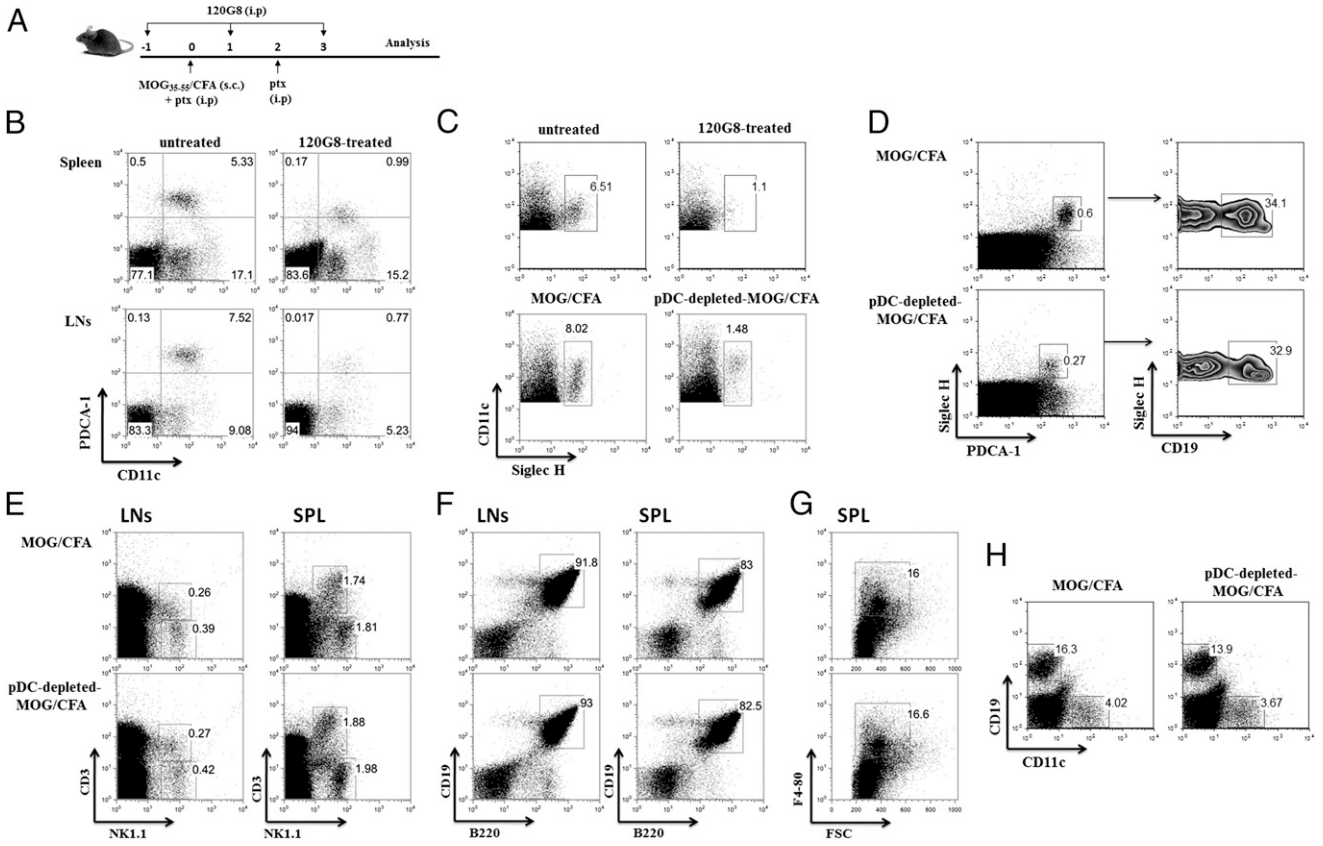

FIGURE 1. In vivo administration of 120G8 mAb specifically eliminates pDCs from the peripheral lymphoid compartment of MOG/CFA immunized animals. (**A**) Experimental protocol of pDC depletion in mice during EAE priming. C57/BL6 female mice were immunized with MOG/CFA at day 0 and received i.p. injections of the 120G8 mAb at days −1, 1, and 3. (**B**) Spleens and LNs were collected from 120G8-treated or untreated nonimmunized C57/BL6 mice 1 d after the last injection of pDC-depleting Ab and analyzed by flow cytometry for the presence of pDCs, based on the expression of PDCA-1 and CD11c markers ($PDCA1^+CD11c^{low}$). Percentages indicate frequency, and gates were set on $7AAD^-CD3^-CD19^-CD11b^-$ cells. (**C**) LNs were collected as indicated earlier and were analyzed by flow cytometry for SiglecH and CD11c (gates were set on total $CD11c^+$ cells). (**D**) dLNs from pDC-depleted and control immunized mice were assessed for the presence of CD19-expressing pDCs (gates on left panel were set on $SiglecH^+PDCA1^+$ cells). Assessment of the frequency of (**E**) NK and NKT cells (gates were set in total LN and spleen cells), (**F**) $CD19^+B220^+$ B cells (gates were set on $CD3^-CD11b^-$ cell populations), and (**G**) $CD11b^+F4/80^+$ macrophages (gates were set on $B220^-CD11c^-$ cells) in the peripheral lymphoid organs of pDC-depleted and control immunized mice 4 d after the antigenic challenge. (**H**) Flow cytometric analysis of BM cells from pDC-depleted and control immunized mice for the presence of $CD19^+$ B cells and $CD11c^+$ DCs (gates were set upon analysis of the entire BM). Mice (n = 3–4) were analyzed individually; data are representative of at least two independent experiments.

$CD11b^+F4/80^+$ macrophages (Fig. 1G, gates were set on $B220^-$ $CD11c^-$ cells) in the spleen and LNs of pDC-depleted as compared with control immunized mice, 4 d after the antigenic challenge. In addition, flow cytometric analysis revealed a slight decrease in the frequency of $CD19^+$ cells, but not in $CD11c^+$ DCs, in the BM of pDC-depleted mice compared with control animals (Fig. 1H, gates were set upon analysis of the entire BM). Collectively, these findings indicate that administration of 120G8 mAb in MOG/CFA immunized animals specifically deplete pDCs from the peripheral lymphoid compartments.

In vivo depletion of pDCs ameliorates the severity and onset of EAE and impairs the priming of myelin-specific T cells in the dLNs

We next addressed the effect of pDC depletion on the development of EAE. To this end, depletion of pDCs during MOG/CFA immunization resulted in delayed onset (15 ± 1.5 versus 10 ± 1.9 d) and less severe course of EAE (maximum severity: 1.07 ± 0.6 versus 2.93 ± 1.2; $*p \leq 0.05$, $**p \leq 0.02$) compared with MOG/CFA immunized control mice (Fig. 2A). Histopathological analysis of spinal cords demonstrated markedly reduced inflammation

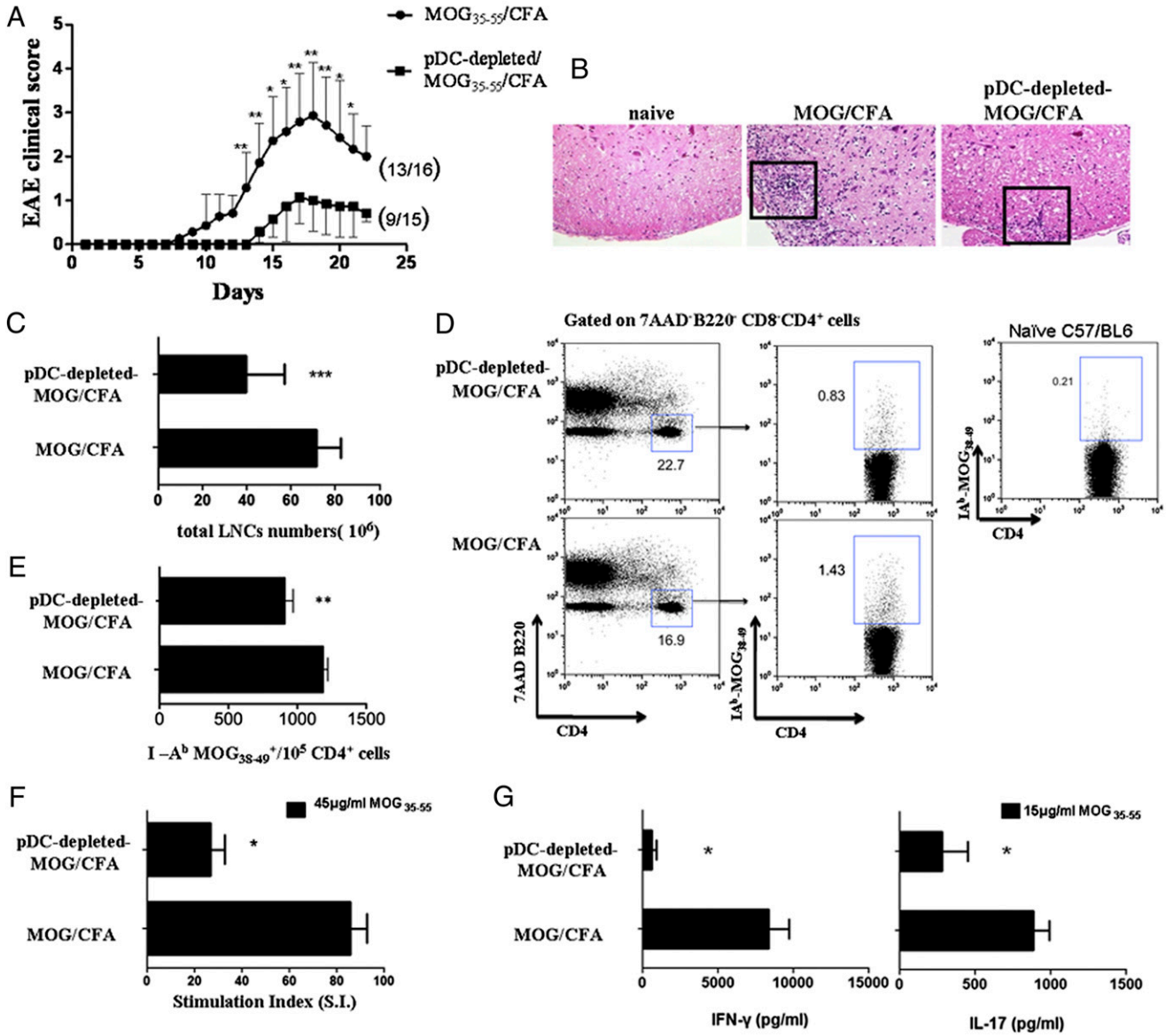

FIGURE 2. Depletion of pDCs ameliorates EAE and inhibits the priming of autoantigen-specific T cells. (**A**) Mean clinical score of EAE in pDC-depleted MOG/CFA and MOG/CFA-immunized mice (controls). Numbers in parentheses represent affected/total mice (n = 15–16/group). Data are representative of two independent experiments ($*p \leq 0.05$, $**p \leq 0.02$). (**B**) Immunohistological analysis of spinal cords isolated from the indicated groups of mice, 14 d after the antigenic challenge. Inflammatory cell infiltration is indicated by H&E staining (original magnification ×400). Results are representative of two to three independent experiments. (**C**) Mice (n = 3–4) were sacrificed 9 d after immunization and dLNs were excised. Bars represent the total lymph node cell (LNC) numbers in control and pDC-depleted MOG/CFA immunized mice group ($***p = 0.0005$). (**D** and **E**) Frequency and absolute numbers of MOG-specific $CD4^+$ T cells in pDC-depleted MOG/CFA and control immunized mice was determined upon staining of LNCs with IA^b-$MOG_{38–49}$ tetramer. Dot plots (D) depict percentages and bars (E) represent absolute numbers of tetramer$^+7AAD^-B220^-CD8^-CD4^+$ T cells ($**p$ = 0.0044). (**F** and **G**) LNCs cultured in the presence or absence of $MOG_{35–55}$ peptide (15 or 45 μg/ml). Eighteen hours before harvesting, 1 μCi [^{3}H] was added, and incorporated radioactivity was measured. Results are expressed as S.I. (cpm in the presence of Ag/cpm in the absence of Ag); $*p = 0.0149$. (G) Mice were analyzed individually; data are representative of at least two independent experiments. Culture supernatants were collected 48 h after culture and assessed for the presence of IFN-γ ($*p = 0.024$) and IL-17 ($*p = 0.04$) by ELISA.

in pDC-depleted MOG/CFA-immunized mice compared with control group (Fig. 2B). Together, these data indicate that depletion of pDCs during the priming of the autoimmune response results in significant alleviation of EAE.

Because T cells play an indispensable role in the initiation of the autoimmune response during EAE, we examined how pDC ablation affected the priming and expansion of autoreactive myelin-specific T cells in the dLNs. To this end, depletion of pDCs significantly reduced the total cell numbers of dLNs compared with the untreated group (41.29 ± 4.848 versus $71.61 \pm 4.118 \times 10^6$ cells; $^{***}p = 0.0005$; Fig. 2C) 9 d after the MOG immunization. Furthermore, ex vivo staining of $CD4^+$ T cells with $MOG_{38–49}/IA^b$ tetramer revealed decreased frequency (Fig. 2D) as well as reduced absolute numbers (Fig. 2E) of MOG-specific T cells in dLNs of pDC-depleted mice compared with control group (909 ± 60.95 versus $1186 \pm 35.53/10^5$ $CD4^+$ T cells; $^{**}p = 0.0044$). Background tetramer staining was determined upon incubation of inguinal LNs from naive mice with $MOG_{38–49}/IA^b$ tetramer and flow cytometry analysis (Fig. 2D). Finally, in vitro antigenic stimulation of dLNs from pDC-treated mice demonstrated an impaired proliferation of MOG-specific T cells (S.I.: 20.28 ± 2.116 versus 78.94 ± 6.932; $^{*}p = 0.0149$; Fig. 2F) and decreased production of IFN-γ and IL-17 compared with nontreated mice (IFN-γ: 895.5 ± 104.5 versus 8333 ± 1375, $^{*}p = 0.024$; IL-17: 280.7 ± 171 versus 882.6 ± 105.4, $^{*}p = 0.04$; Fig. 2G). Collectively, depletion of pDCs in EAE mice during the initiation phase inhibits the priming of autoreactive T cells in the dLNs.

$Foxp3^+$ Treg homeostasis and cDC migration to peripheral LNs are not affected by pDC depletion

It has been demonstrated that pDCs could facilitate the induction and expansion of Tregs (3). To examine whether the impaired priming of autoreactive T cells upon pDC depletion could be attributed to alterations of Treg homeostasis, we assessed the frequency of $CD4^+$ $Foxp3^+$ T cells in the peripheral lymphoid organs of pDC-depleted Foxp3-GFP mice. As shown in Fig. 3A, no significant differences in the frequency of $CD4^+Foxp3^+$ ($7AAD^-CD19^-CD8^-$) Treg cells were observed in the dLNs of the two groups of mice, either at day 0, before the antigenic challenge, or 9 d after the pDC depletion and MOG immunization. Alternatively, pDC depletion might affect the recruitment and/or Ag presentation of cDCs in the dLNs. Thus, we assessed the frequency of $CD11c^+$ cDCs ($7AAD^-CD3^-CD19^-PDCA\text{-}1^-$) in the dLNs at the same time points as described earlier, and we observed similar accumulation of cDCs between control and pDC-depleted mice (Fig. 3B). Furthermore, immunization of pDC-depleted and control mice with fluorochrome-conjugated OVA in CFA demonstrated that absence of pDCs did not affect the ability of cDCs to uptake Ag as indicated by the induction of the green fluorescent label (Fig. 3C). Finally, we examined whether pDC depletion affected the levels of CCL19 and CCL21 by stromal cells. Both chemokines play an important role in the priming of the immune response because they are involved in the trafficking of T cells and DCs in the T cell areas of the LNs (32). LN homogenates isolated from either pDC-depleted or control mice

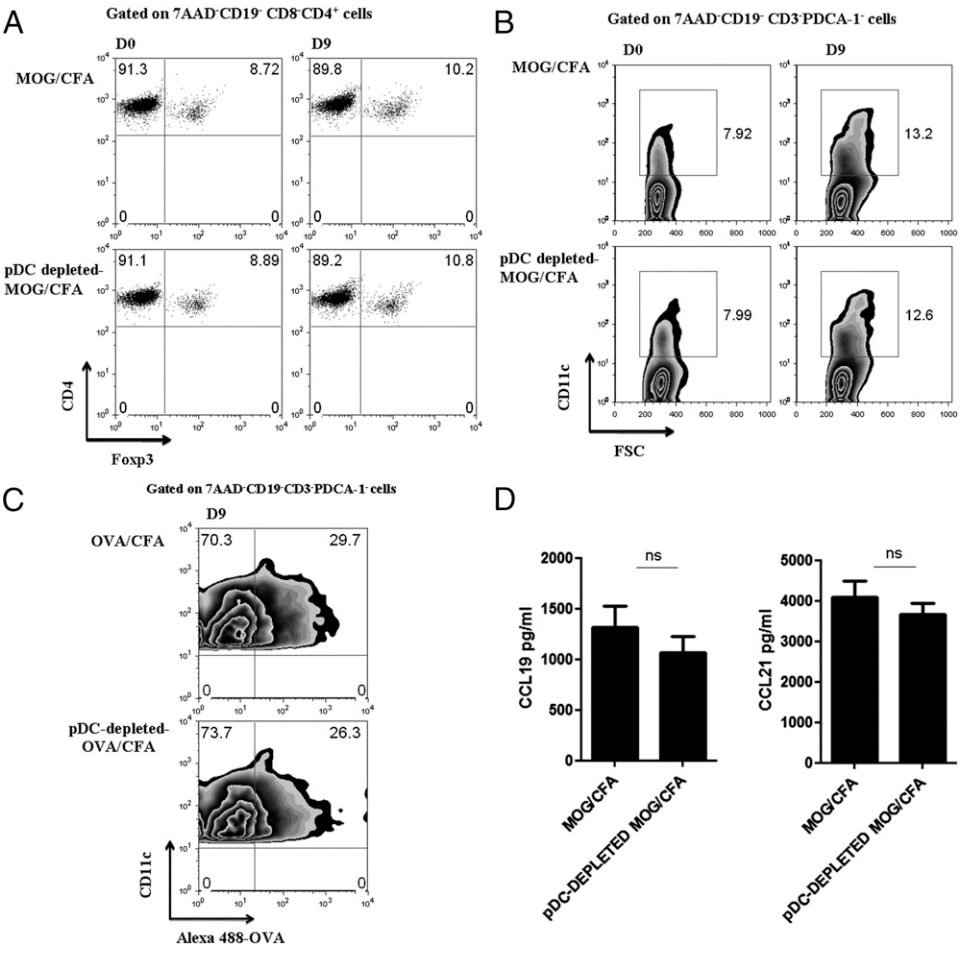

FIGURE 3. Absence of pDCs does not affect the frequency of $Foxp3^+$ Tregs or cDCs in the dLNs. (**A**) dLNs from MOG/CFA and pDC-depleted MOG/CFA immunized mice (Foxp3GFP-C57/BL6; $n = 3$), were isolated at day 9 after immunization and analyzed for the frequency of $CD4^+$ $Foxp3^+(GFP^+)$ T cells by FACS analysis. Gates were set on $7AAD^-CD19^-CD8^-CD4^+$ cells. (**B**) dLNs were isolated from pDC-depleted MOG/CFA and control mice ($n = 3$–4), 9 d after antigenic challenge, and analyzed for the frequency of cDCs based on the expression of CD11c. Numbers indicate percentages, and gates were set on $7AAD^-CD19^-CD3^-PDCA\text{-}1^-$ cells. (**C**) Mice were immunized with Alexa 488–conjugated OVA (100 μg/mouse; $n = 3$). Nine days after immunization, dLN cells from OVA/CFA or pDC-depleted OVA/CFA stained with DC-specific markers and Ag uptake (Alexa 488–conjugated OVA) were measured using flow cytometric analysis. Plots show the frequency of cDCs that uptake OVA, which are the $CD11c^+OVA^+$ cells. Gates were set on $7AAD^-CD19^-CD3^-PDCA\text{-}1^-$ cells. (**D**) Detection of CCL19/CCL21 levels in dLN homogenates at day 4 after immunization by sandwich ELISA. Data are representative of three independent experiments. ns, Nonsignificant.

did not demonstrate any significant difference on CCL19 and CCL21 protein levels (Fig. 3D). Collectively, these data suggest that pDC depletion does not alter the Treg homeostasis or the migration and functional properties of cDCs in the dLNs. Therefore, other mechanisms should operate that contribute to the impaired priming of autoreactive T cells and the subsequent amelioration of the autoimmune response upon pDC depletion.

Increased myelopoiesis in the BM and release of CD11b^{hi}Gr1^{+} MDSCs in the periphery of pDC-depleted mice

It was previously demonstrated that lack of cDCs induces a myeloid-proliferative disorder characterized by increased generation of myeloid cells in the BM (33). To investigate whether pDC depletion affects myelopoiesis, we analyzed BM cells from pDC-depleted control mice, as well as cDC-depleted mice, for the frequency of myeloid cell populations. Interestingly, we found that depletion of pDCs caused a slight but significant increase of the frequency (Fig. 4A) and absolute numbers (Fig. 4B) of CD11b^{hi} Gr1$^{hi/int}$ cells in the BM as compared with control mice ($301 \times 10^3 \pm 4.163$ versus $254.3 \times 10^3 \pm 9.871$; $^{*}p = 0.0121$), whereas the increase of CD11b^{hi}Gr1$^{hi/int}$ cells was more profound upon cDC depletion ($496 \times 10^3 \pm 30.39$ versus $254.3 \times 10^3 \pm 9.871$; $^{**}p = 0.0016$). These data suggest that pDC depletion, during an inflammatory response, augments myelopoiesis in the BM and more specifically the frequency of the CD11b^{hi}Gr1$^{hi/int}$ cell subset.

The phenotype of this cell subset is consistent with the MDSCs that have demonstrated to potently suppress ongoing T cell responses in cancer and autoimmunity (25, 27, 34). To further assess whether increased CD11b^{hi}Gr1^{+} MDSCs could account for the impaired priming of the autoimmune response, we examined the presence of CD11b^{hi}Gr1^{+} MDSCs in the peripheral lymphoid compartments. Analysis of the spleen from pDC-depleted MOG/CFA immunized mice revealed a significant increase of CD11b^{hi} Gr1^{+} (7AAD^{-}) MDSCs in frequency (Fig. 5A) and absolute numbers ($60{,}750 \pm 3511$ versus $35{,}520 \pm 6883/10^6$ splenocytes; $^{*}p = 0.017$; Fig. 5B) compared with control immunized mice either 4 or 9 d after the immunization. We next examined the frequency of MDSCs in the dLNs of pDC-depleted MOG/CFA-immunized mice, and we observed an increased accumulation of CD11b^{hi}Gr1^{+} cells as compared with the control group that was more profound on day 9 after immunization (Fig. 5C). The increased accumulation of CD11b^{hi}Gr1^{+} cells in the spleen of pDC-depleted mice could be caused by continued release from the BM or local expansion in the spleen. To address this, we injected pDC-depleted MOG/CFA immunized and control mice with BrdU at day 4 after immunization, and 4 h later, we determined BrdU incorporation by MDSCs. As shown in Fig. 5D, no DNA synthesis by CD11b^{hi} Gr1^{+} cells was observed in the spleen of pDC-depleted or control animals, whereas BrdU incorporation was prominent in CD4^{+} thymocytes (positive control, data not shown). These data indicate that the increased accumulation of MDSCs at the peripheral lymphoid organs during pDC depletion is due to their continuous egress from the BM rather than expansion in the site of inflammation.

MDSCs from pDC-depleted mice potently suppress the proliferation of naive CD4^{+} T cells in vitro

To investigate whether the suppressive function of MDSCs is affected by pDC depletion, we activated naive CFSE-labeled CD4^{+} CD25^{-} T cells in vitro with anti-CD3/anti-CD28 and cocultured them in the presence of MDSCs sorted from the spleens of pDC-depleted or control mice (purity $> 95\%$). MDSCs isolated from pDC-depleted mice suppressed the proliferation of T cells to the same extent as MDSCs isolated from control-immunized mice (Fig. 6), indicating that the suppressive potential of MDSCs is not altered upon pDC depletion.

Type I IFNs do not affect the recruitment or expansion of MDSCs during the priming of the autoimmune response

Under inflammatory situations, pDCs release large quantities of type I IFN, which is a hallmark of pDC activation (35). To address a potential role of type I IFNs in MDSC accumulation in the spleen of MOG/CFA-immunized mice, we administered IFN-β during the initiation of the autoimmune response (daily injections from days 0–5). Flow-cytometric analysis at day 6 demonstrated no difference in the frequency and absolute numbers of MDSCs in IFN-β–treated mice as compared with untreated control group (Fig. 7). Thus, reduced levels of type I IFN are unlikely to account for the increased release of MDSCs in the periphery of pDC-depleted mice.

MCP-1 induces accumulation of MDSCs in the peripheral lymphoid organs

During inflammation, myeloid cells are constantly expanded and released from the BM in the periphery, in response to various signals. An important chemokine that has been shown to facilitate

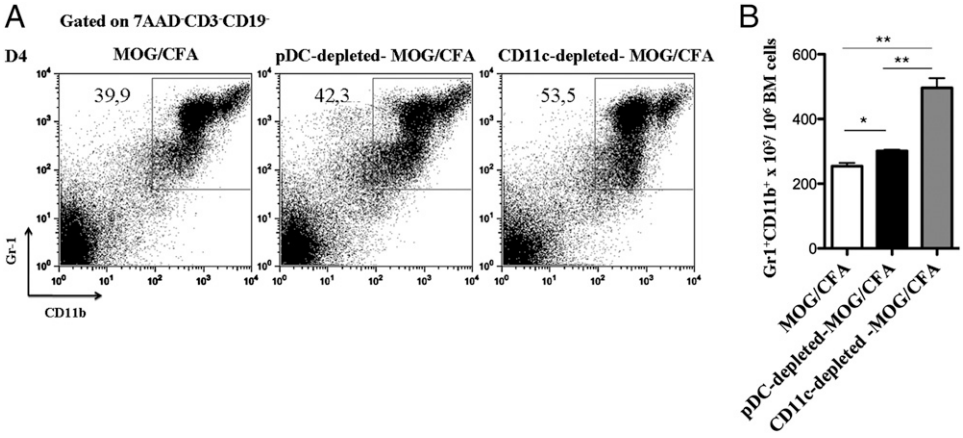

FIGURE 4. pDC depletion promotes the expansion of CD11b^{hi}Gr1^{+} MDSCs in the BM and their release in the peripheral lymphoid organs. (**A** and **B**) BM cells were collected from MOG/CFA, pDC-depleted, or CD11c-depleted MOG/CFA immunized mice ($n = 4$) 4 d after immunization and analyzed by flow cytometry for the presence of CD11b^{hi}Gr1^{+} MDSCs. (A) Frequency and (B) absolute numbers of MDSCs in BM cells isolated from the aforementioned groups. Gates were set on 7AAD^{-}CD3^{-}CD19^{-} cells. Mice were analyzed individually; data are representative of at least two independent experiments. pDC depleted: $^{*}p = 0.0121$, cDC depleted, and $^{**}p = 0.0016$.

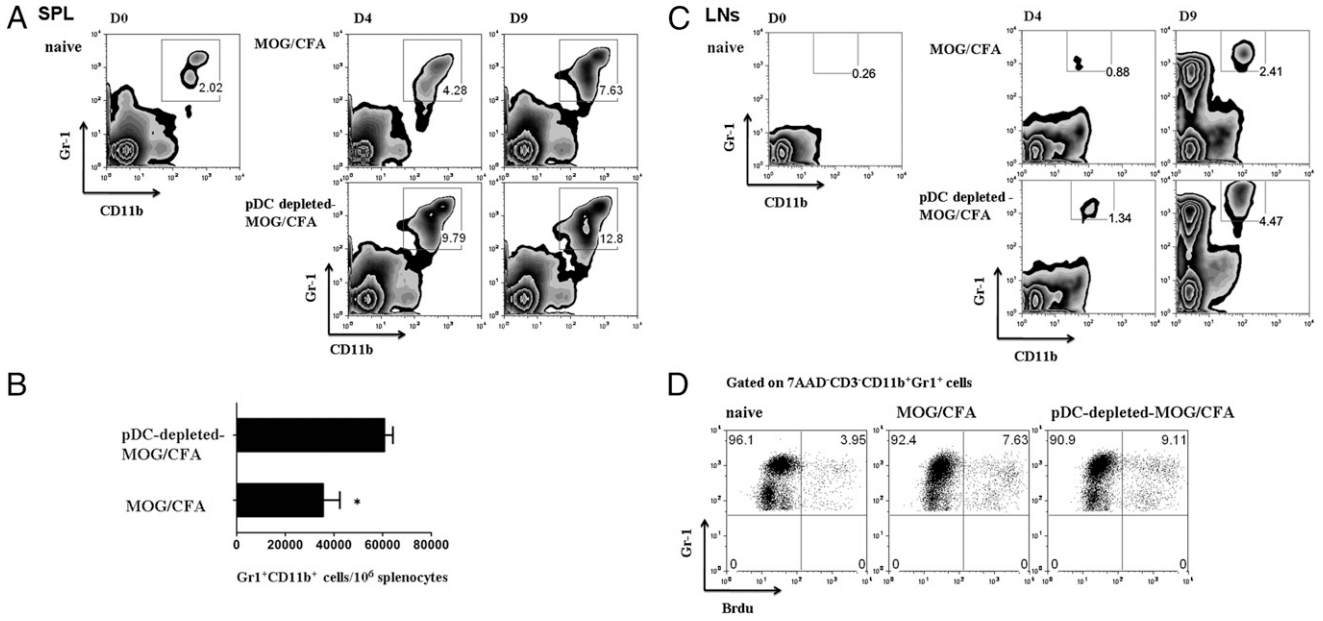

FIGURE 5. pDC depletion leads to accumulation of MDSCs in the peripheral lymphoid organs. (**A**) Splenocytes and (**C**) dLNs from pDC-depleted and control MOG/CFA immunized mice were analyzed for the presence of $CD11b^{hi}Gr1^{+}$ (MDSCs) at different time points (days 4 and 9 after immunization, respectively). Numbers show percentage of cells. (**B**) Absolute numbers of MDSCs in the spleens of control and pDC-depleted mice 9 d after immunization, $*p = 0.017$. (**D**) BrdU incorporation by MDSCs in the spleen of MOF/CFA immunized mice 4 d after immunization. Representative flow cytometric analysis indicates percentages of $BrdU^{-}$ or $BrdU^{+}$ cells in the corresponding gates. Gates were set as indicated. Results are representative of two independent experiments with two mice per group.

the egress of myeloid cells from the BM is MCP-1 (MCP-1/CCL-2) (36). Therefore, we hypothesized that pDC depletion increases the levels of MCP-1 in the periphery, and thus the emigration of MDSCs in the spleen of immunized mice. To this end, we examined the levels of MCP-1 in LN homogenates isolated from pDC-depleted MOG/CFA-immunized and control immunized animals. Interestingly, MCP-1 levels were significantly increased in pDC-depleted MOG/CFA-immunized mice compared with control mice (446.3 ± 48.6 versus 216.8 ± 20.48 pg/ml; $**p = 0.0024$; Fig. 8A). To provide direct evidence for the role of MCP-1 in the emigration of MDSCs from the BM to the periphery, we administered i.p. rMCP-1 in MOG/CFA immunized mice and determined the MDSC frequency. As shown in Fig. 8B and 8C, MCP-1–treated mice showed significantly increased recruitment of MDSCs in the peripheral blood and spleen when compared with the control group (blood: 31,530 ± 4563 versus 13,310 ± 2233/5 × 10^5 PBMCs, $*p = 0.011$; spleen: 49,310 ± 2257 versus 38,760 ± 2518/5 × 10^5 splenocytes, $*p = 0.02$).

This finding suggests that accumulation of MDSCs in the peripheral lymphoid organs of MOG/CFA-immunized mice is mediated by MCP-1. Whether other factors could also influence the migration of MDSCs from the BM to the periphery of mice during an autoimmune response needs to be further investigated.

Discussion

In this study, we demonstrate that elimination of pDCs during the priming phase of EAE results in amelioration of disease pathology and impaired priming of autoreactive T cells in the dLNs. The

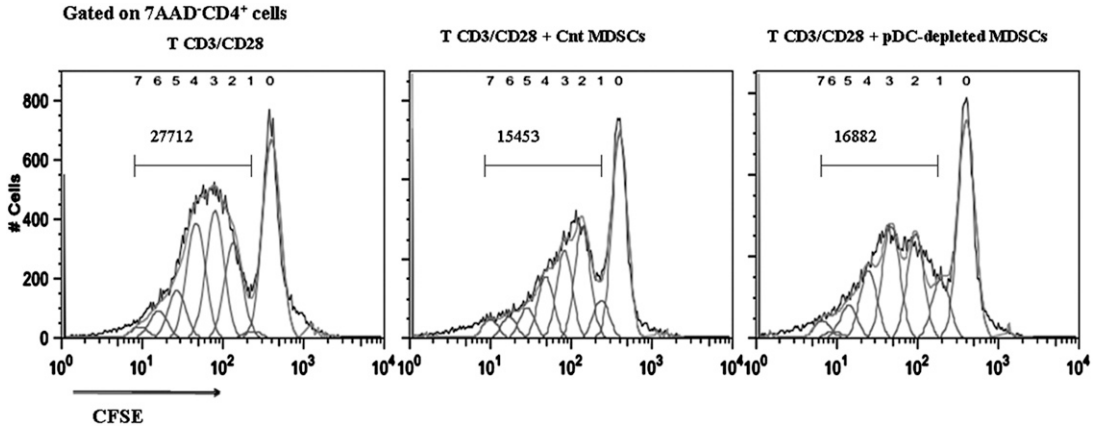

FIGURE 6. MDSCs isolated from the spleen of pDC-depleted mice efficiently suppress the proliferation of naive $CD4^{+}$ T cells. $CD4^{+}CD25^{-}$ T cells were sorted (purity > 99%) from spleens of naive mice, labeled with CFSE, and cultured (5 × 10^5/well) in the presence of plate-bound anti-CD3 (10 μg/ml) and anti-CD28 (1 μg/ml). Sorted MDSCs (purity > 95%) from spleens of MOG/CFA or pDC-depleted MOG/CFA immunized mice (two mice/group) were added in the cultures in 1:1 ratio. Proliferation of T cells was assessed based on CFSE dilution (gates were set on $7AAD^{-}CD4^{+}$ cells). Values represent the number of $CD4^{+}$ T cells that have undergone division, in the absence of MDSCs (*left panel*) and in the presence of MDSCs isolated either from MOG/CFA mice (*middle panel*) or pDC-depleted MOG/CFA mice (*right panel*). Data are representative of three independent experiments.

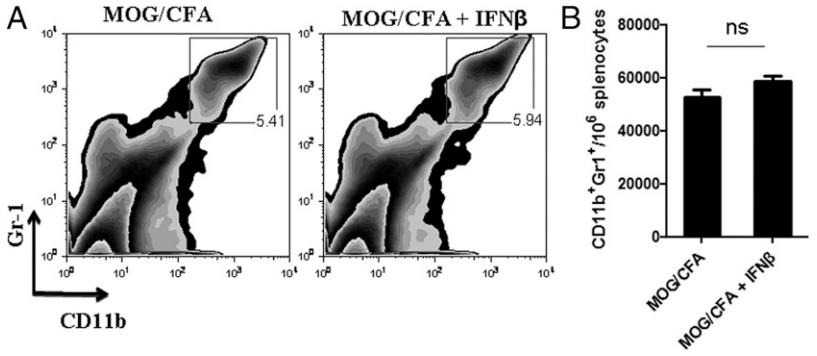

FIGURE 7. Administration of IFN-β does not affect the accumulation of MDSCs in the periphery of MOG/CFA immunized mice. (**A** and **B**) MOG/CFA immunized mice treated daily with 2 μg rIFN-β (Rebif) from days 0–5. At day 6, mice sacrificed and analyzed by flow cytometry for the frequency of MDSCs in the periphery. (A) Frequency and (B) absolute numbers of MDSCs in the spleen of control or IFN-β–treated mice. Data are representative of two independent experiments. Each mouse was analyzed individually (n = 5/group). ns, Nonsignificant.

findings presented in this article are in line with the observations by Isaksson et al. (24) where treatment of mice with anti-PDCA1 during the induction of EAE inhibited disease development. Moreover, our data describe a mechanism that links pDCs with MDSCs and disease suppression. Our results support the notion of distinct innate and adaptive functions of pDCs because in other studies, depletion of pDCs during the onset of EAE or the acute phase of experimental arthritis exacerbated disease (21, 22). Collectively, based on the distinct roles of pDCs during the initiation, progression, and effector phase of EAE, we propose that selective elimination of pDCs might be superior to a long-term pDC ablation, to elucidate the role of this cell subset during autoreactive T cell priming.

Activation of myelin-specific Th1 and Th17 cells in the LNs is the first step of the autoimmune cascade during EAE. We show in this article that depletion of pDCs before the MOG/CFA priming results in reduced frequency of MOG-specific T cells in dLNs and significantly decreased levels of IFN-γ and IL-17 in recall in vitro assays. The inefficient priming of autoreactive myelin-specific T cells in pDC-depleted mice could be explained by several mutually nonexclusive hypotheses. First, soluble factors that are secreted by activated pDCs have been shown to "orchestrate" the cDC-mediated T cell activation (37, 38). Therefore, pDC ablation might inhibit the proper migration of cDCs in the dLNs and/or their ability to present Ags. In our experimental system, we ruled out this possibility because we demonstrated that the migration of Ag-bearing cDCs to the dLNs is not affected by the absence of pDCs. Second, pDCs have the capacity to uptake, process, and present Ags to $CD4^+$ T cells (4, 6); therefore, their absence could affect T cell priming. Whether this mechanism is involved in the amelioration of EAE upon pDC depletion in the initiation phase of disease remains to be elucidated.

An indispensable role of pDCs in the induction of Tregs, and thus in the maintenance of immune tolerance, has been established in several experimental mouse models (8–11), as well as human samples (13). In CNS autoimmunity, it has been demonstrated that myelin-presenting pDCs promote the expansion of $Foxp3^+$ Tregs, and thus the induction of dominant tolerance and amelioration of EAE (23). In contrast, it was recently reported that myelin Ag targeting to pDCs via siglecH did not facilitate Treg induction (neither natural Tregs nor T regulatory 1), but instead induced a hyporesponsive state in $CD4^+$ T cells and inhibition of EAE

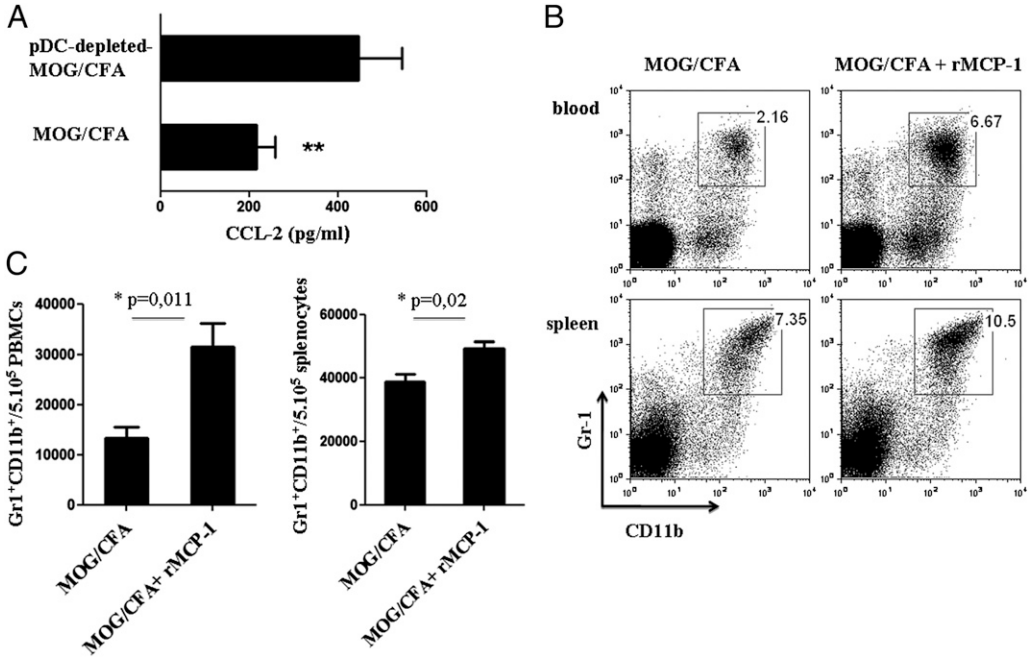

FIGURE 8. MCP-1 induces the accumulation of MDSCs in the peripheral lymphoid organs. (**A**) Control and pDC-depleted MOG/CFA immunized mice (n = 3–4) sacrificed 4 d after immunization and dLN homogenates were analyzed for MCP-1 levels by ELISA. $^{**}p$ = 0.002. (**B** and **C**) MOG/CFA immunized mice were injected i.p. with rMCP-1 (1000 ng/mouse), and MDSC accumulation in peripheral blood and spleen was analyzed by flow cytometry. Frequency (B) and absolute numbers (C) of MDSCs accumulated in the control or chemokine-treated mice in blood (*upper panel*) and spleen (*lower panel*). Mice were analyzed individually; data are representative of at least two independent experiments. $^*p$ = 0.011 (*left panel*), $^*p$ = 0.02 (*right panel*).

pathology (39). Our data demonstrated that depletion of pDCs during the MOG/CFA immunization did not alter the frequency of Foxp3-expressing Tregs in the dLNs, suggesting that other APCs might be involved in the maintenance and/or expansion of Tregs under the specific inflammatory milieu. In support of this notion, it was shown that under steady-state, homeostatic proliferation of Tregs was not solely dependent on pDCs (40). Moreover, cell types other than pDCs have been shown to instruct the expansion and induction of $Foxp3^+$ Tregs in vivo (41–43).

The immunosuppressive properties of MDSCs have been well characterized in the immune responses in cancer and in bacterial or parasitic infections (44–49), and recently we reported their crucial role in suppressing CNS autoimmune responses (27). MDSCs are constantly released form the BM into the periphery under inflammatory situations and, depending on the specific microenvironment, could either exert inhibitory functions or could differentiate into DCs, macrophages, and neutrophils (25, 50). The molecules that mediate their egress from the BM, their migration dynamics, as well as their differentiation properties remain to be established. Our results demonstrate that depletion of pDCs significantly increased myelopoiesis in the BM and the frequency of $CD11b^{hi}Gr1^+$ MDSCs in the spleen of MOG/CFA immunized mice. In line with our findings, constitutive ablation of cDCs results in a dramatic increase of myeloid cell generation in the BM and the development of myeloid proliferative syndrome (33). Taken together, we hypothesize that absence of pDCs induces a compensatory mechanism that triggers myelopoiesis in the BM, and thus increased generation of MDSCs. The increased accumulation of MDSCs in the spleen of pDC-depleted mice could be attributed to a cell proliferation in response to autoimmune stimuli. Indeed, it has been reported that MDSCs are able to proliferate in a tumor model (51). In contrast, our results show that only a minor proportion of $CD11b^{hi}Gr1^+$ MDSCs incorporate BrdU during MOG/CFA immunization, indicating that MDSCs do not proliferate in the periphery, under the specific autoimmune environment. Therefore, the increased accumulation of MDSCs in the spleen during EAE is mainly due to constant release of these cells from the BM.

Inflammatory situations are characterized by increased trafficking of myeloid cells into the peripheral blood and tissues, and the precise mechanism involved in the mobilization of such cells is ill-defined. Among the different mediators that have been involved in such a process, chemokines have been shown to play a predominant role (52, 53). To delineate the mechanism involved in the increased emigration of MDSCs in the spleen of pDC-depleted mice, we focused on MCP-1 because: 1) it has been involved in the recruitment of myeloid suppressor cells into tumors (54), and 2) it was demonstrated that chemokine receptor 2 (CCR2) expression (which specifically binds MCP-1) was required for the migration of monocytic cells from the BM during *L. monocytogenes* infection (36). Interestingly, we observed a significant increase of MCP-1 secretion in the dLNs of pDC-depleted MOG/CFA mice as compared with control immunized animals. Notably, we were not able to detect increased levels of mcp-1 in spleen homogenates of pDC-depleted and control immunized mice. This could possibly be explained by the broad distribution of cell types, as well as the abundance of variable soluble factors in the spleen. Importantly, administration of rMCP-1 in immunized animals caused increased mobilization of $CD11b^{hi}Gr1^+$ MDSCs in the blood and spleen compared with untreated animals. Taken together, these data provide an additional mechanism of regulation of the autoimmune response through the increase of MCP-1 levels in the periphery of MOG/CFA immunized mice. The mechanism through which pDC depletion results in increased MCP-1 secretion requires further investigation. One possible hypothesis could be that upon activation, pDCs secrete soluble mediators that regulate MCP-1 secretion by stromal or other cells. Indeed, we isolated by cell sorting several cell populations from the dLNs of pDC-depleted and control immunized mice, and analyzed by PCR for expression of MCP-1. We found increased expression of mcp-1 in the $CD45^-$ cell population (which includes stromal cells), but the differences did not reach statistical significance (data not shown). Isolation of specific stromal cell populations (i.e., fibroblastic reticular cells or reticular endothelial cells) might provide evidence for the cellular source of mcp-1 in pDC-depleted mice in this autoimmune setting. Therefore, absence of pDCs results in increased MCP-1 production, and this facilitates the mobilization of MDSCs from the BM to the periphery. This increased mobilization of MDSCs might account for the inhibition of the autoreactive immune response and subsequent amelioration of EAE.

A better understanding of the molecular mechanisms that govern the expansion and mobilization of MDSCs in the periphery during an autoimmune response would provide meaningful insights in the functional properties of this powerful suppressor cell subset that could be explored therapeutically.

Acknowledgments

We thank Z. Vlata and N. Gounalaki for technical assistance with cell sorting and A. Agapaki (Biomedical Research Foundation of the Academy of Athens) for histology preparations.

Disclosures

The authors have no financial conflicts of interest.

References

1. Shortman, K., and S. H. Naik. 2007. Steady-state and inflammatory dendritic-cell development. *Nat. Rev. Immunol.* 7: 19–30.
2. Colonna, M., G. Trinchieri, and Y. J. Liu. 2004. Plasmacytoid dendritic cells in immunity. *Nat. Immunol.* 5: 1219–1226.
3. Reizis, B., A. Bunin, H. S. Ghosh, K. L. Lewis, and V. Sisirak. 2011. Plasmacytoid dendritic cells: recent progress and open questions. *Annu. Rev. Immunol.* 29: 163–183.
4. Villadangos, J. A., and L. Young. 2008. Antigen-presentation properties of plasmacytoid dendritic cells. *Immunity* 29: 352–361.
5. Hoeffel, G., A. C. Ripoche, D. Matheoud, M. Nascimbeni, N. Escriou, P. Lebon, F. Heshmati, J. G. Guillet, M. Gannagé, S. Caillat-Zucman, et al. 2007. Antigen crosspresentation by human plasmacytoid dendritic cells. *Immunity* 27: 481–492.
6. Sapoznikov, A., J. A. Fischer, T. Zaft, R. Krauthgamer, A. Dzionek, and S. Jung. 2007. Organ-dependent in vivo priming of naive CD4+, but not CD8+, T cells by plasmacytoid dendritic cells. *J. Exp. Med.* 204: 1923–1933.
7. Di Pucchio, T., B. Chatterjee, A. Smed-Sörensen, S. Clayton, A. Palazzo, M. Montes, Y. Xue, I. Mellman, J. Banchereau, and J. E. Connolly. 2008. Direct proteasome-independent cross-presentation of viral antigen by plasmacytoid dendritic cells on major histocompatibility complex class I. *Nat. Immunol.* 9: 551–557.
8. Ochando, J. C., C. Homma, Y. Yang, A. Hidalgo, A. Garin, F. Tacke, V. Angeli, Y. Li, P. Boros, Y. Ding, et al. 2006. Alloantigen-presenting plasmacytoid dendritic cells mediate tolerance to vascularized grafts. *Nat. Immunol.* 7: 652–662.
9. de Heer, H. J., H. Hammad, T. Soullié, D. Hijdra, N. Vos, M. A. Willart, H. C. Hoogsteden, and B. N. Lambrecht. 2004. Essential role of lung plasmacytoid dendritic cells in preventing asthmatic reactions to harmless inhaled antigen. *J. Exp. Med.* 200: 89–98.
10. Sharma, M. D., B. Baban, P. Chandler, D. Y. Hou, N. Singh, H. Yagita, M. Azuma, B. R. Blazar, A. L. Mellor, and D. H. Munn. 2007. Plasmacytoid dendritic cells from mouse tumor-draining lymph nodes directly activate mature Tregs via indoleamine 2,3-dioxygenase. *J. Clin. Invest.* 117: 2570–2582.
11. Manches, O., D. Munn, A. Fallahi, J. Lifson, L. Chaperot, J. Plumas, and N. Bhardwaj. 2008. HIV-activated human plasmacytoid DCs induce Tregs through an indoleamine 2,3-dioxygenase-dependent mechanism. *J. Clin. Invest.* 118: 3431–3439.
12. Chen, W., X. Liang, A. J. Peterson, D. H. Munn, and B. R. Blazar. 2008. The indoleamine 2,3-dioxygenase pathway is essential for human plasmacytoid dendritic cell-induced adaptive T regulatory cell generation. *J. Immunol.* 181: 5396–5404.
13. Kavousanaki, M., A. Makrigiannakis, D. Boumpas, and P. Verginis. 2010. Novel role of plasmacytoid dendritic cells in humans: induction of interleukin-10-producing Treg cells by plasmacytoid dendritic cells in patients with rheumatoid arthritis responding to therapy. *Arthritis Rheum.* 62: 53–63.

14. Rönnblom, L., M. L. Eloranta, and G. V. Alm. 2003. Role of natural interferon-alpha producing cells (plasmacytoid dendritic cells) in autoimmunity. *Autoimmunity* 36: 463–472.
15. Rönnblom, L., and G. V. Alm. 2001. A pivotal role for the natural interferon alpha-producing cells (plasmacytoid dendritic cells) in the pathogenesis of lupus. *J. Exp. Med.* 194: F59–F63.
16. Jahnsen, F. L., L. Farkas, F. Lund-Johansen, and P. Brandtzaeg. 2002. Involvement of plasmacytoid dendritic cells in human diseases. *Hum. Immunol.* 63: 1201–1205.
17. Guiducci, C., C. Tripodo, M. Gong, S. Sangaletti, M. P. Colombo, R. L. Coffman, and F. J. Barrat. 2010. Autoimmune skin inflammation is dependent on plasmacytoid dendritic cell activation by nucleic acids via TLR7 and TLR9. *J. Exp. Med.* 207: 2931–2942.
18. Nestle, F. O., C. Conrad, A. Tun-Kyi, B. Homey, M. Gombert, O. Boyman, G. Burg, Y. J. Liu, and M. Gilliet. 2005. Plasmacytoid predendritic cells initiate psoriasis through interferon-alpha production. *J. Exp. Med.* 202: 135–143.
19. Farkas, L., K. Beiske, F. Lund-Johansen, P. Brandtzaeg, and F. L. Jahnsen. 2001. Plasmacytoid dendritic cells (natural interferon- alpha/beta-producing cells) accumulate in cutaneous lupus erythematosus lesions. *Am. J. Pathol.* 159: 237–243.
20. Lande, R., D. Ganguly, V. Facchinetti, L. Frasca, C. Conrad, J. Gregorio, S. Meller, G. Chamilos, R. Sebasigari, V. Riccieri, et al. 2011. Neutrophils activate plasmacytoid dendritic cells by releasing self-DNA-peptide complexes in systemic lupus erythematosus. *Sci. Transl. Med.* 3: 73ra19.
21. Bailey-Bucktrout, S. L., S. C. Caulkins, G. Goings, J. A. Fischer, A. Dzionek, and S. D. Miller. 2008. Cutting edge: central nervous system plasmacytoid dendritic cells regulate the severity of relapsing experimental autoimmune encephalomyelitis. *J. Immunol.* 180: 6457–6461.
22. Jongbloed, S. L., R. A. Benson, M. B. Nickdel, P. Garside, I. B. McInnes, and J. M. Brewer. 2009. Plasmacytoid dendritic cells regulate breach of self-tolerance in autoimmune arthritis. *J. Immunol.* 182: 963–968.
23. Irla, M., N. Küpfer, T. Suter, R. Lissilaa, M. Benkhoucha, J. Skupsky, P. H. Lalive, A. Fontana, W. Reith, and S. Hugues. 2010. MHC class II-restricted antigen presentation by plasmacytoid dendritic cells inhibits T cell-mediated autoimmunity. *J. Exp. Med.* 207: 1891–1905.
24. Isaksson, M., B. Ardesjö, L. Rönnblom, O. Kämpe, H. Lassmann, M. L. Eloranta, and A. Lobell. 2009. Plasmacytoid DC promote priming of autoimmune Th17 cells and EAE. *Eur. J. Immunol.* 39: 2925–2935.
25. Gabrilovich, D. I., and S. Nagaraj. 2009. Myeloid-derived suppressor cells as regulators of the immune system. *Nat. Rev. Immunol.* 9: 162–174.
26. Peranzoni, E., S. Zilio, I. Marigo, L. Dolcetti, P. Zanovello, S. Mandruzzato, and V. Bronte. 2010. Myeloid-derived suppressor cell heterogeneity and subset definition. *Curr. Opin. Immunol.* 22: 238–244.
27. Ioannou, M., T. Alissafi, I. Lazaridis, G. Deraos, J. Matsoukas, A. Gravanis, V. Mastorodemos, A. Plaitakis, A. Sharpe, D. Boumpas, and P. Verginis. 2012. Crucial role of granulocytic myeloid-derived suppressor cells in the regulation of central nervous system autoimmune disease. *J. Immunol.* 188: 1136–1146.
28. Zhang, J., A. Raper, N. Sugita, R. Hingorani, M. Salio, M. J. Palmowski, V. Cerundolo, and P. R. Crocker. 2006. Characterization of Siglec-H as a novel endocytic receptor expressed on murine plasmacytoid dendritic cell precursors. *Blood* 107: 3600–3608.
29. Baban, B., P. R. Chandler, M. D. Sharma, J. Pihkala, P. A. Koni, D. H. Munn, and A. L. Mellor. 2009. IDO activates regulatory T cells and blocks their conversion into Th17-like T cells. *J. Immunol.* 183: 2475–2483.
30. Asselin-Paturel, C., G. Brizard, J. J. Pin, F. Brière, and G. Trinchieri. 2003. Mouse strain differences in plasmacytoid dendritic cell frequency and function revealed by a novel monoclonal antibody. *J. Immunol.* 171: 6466–6477.
31. Blasius, A. L., E. Giurisato, M. Cella, R. D. Schreiber, A. S. Shaw, and M. Colonna. 2006. Bone marrow stromal cell antigen 2 is a specific marker of type I IFN-producing cells in the naive mouse, but a promiscuous cell surface antigen following IFN stimulation. *J. Immunol.* 177: 3260–3265.
32. Marsland, B. J., P. Bättig, M. Bauer, C. Ruedl, U. Lässing, R. R. Beerli, K. Dietmeier, L. Ivanova, T. Pfister, L. Vogt, et al. 2005. CCL19 and CCL21 induce a potent proinflammatory differentiation program in licensed dendritic cells. *Immunity* 22: 493–505.
33. Birnberg, T., L. Bar-On, A. Sapoznikov, M. L. Caton, L. Cervantes-Barragán, D. Makia, R. Krauthgamer, O. Brenner, B. Ludewig, D. Brockschnieder, et al. 2008. Lack of conventional dendritic cells is compatible with normal development and T cell homeostasis, but causes myeloid proliferative syndrome. *Immunity* 29: 986–997.
34. Youn, J. I., S. Nagaraj, M. Collazo, and D. I. Gabrilovich. 2008. Subsets of myeloid-derived suppressor cells in tumor-bearing mice. *J. Immunol.* 181: 5791–5802.
35. Gilliet, M., W. Cao, and Y. J. Liu. 2008. Plasmacytoid dendritic cells: sensing nucleic acids in viral infection and autoimmune diseases. *Nat. Rev. Immunol.* 8: 594–606.
36. Serbina, N. V., and E. G. Pamer. 2006. Monocyte emigration from bone marrow during bacterial infection requires signals mediated by chemokine receptor CCR2. *Nat. Immunol.* 7: 311–317.
37. Takagi, H., T. Fukaya, K. Eizumi, Y. Sato, K. Sato, A. Shibazaki, H. Otsuka, A. Hijikata, T. Watanabe, O. Ohara, et al. 2011. Plasmacytoid dendritic cells are crucial for the initiation of inflammation and T cell immunity in vivo. *Immunity* 35: 958–971.
38. Blanco, P., A. K. Palucka, M. Gill, V. Pascual, and J. Banchereau. 2001. Induction of dendritic cell differentiation by IFN-alpha in systemic lupus erythematosus. *Science* 294: 1540–1543.
39. Loschko, J., S. Heink, D. Hackl, D. Dudziak, W. Reindl, T. Korn, and A. B. Krug. 2011. Antigen targeting to plasmacytoid dendritic cells via Siglec-H inhibits Th cell-dependent autoimmunity. *J. Immunol.* 187: 6346–6356.
40. Darrasse-Jèze, G., S. Deroubaix, H. Mouquet, G. D. Victora, T. Eisenreich, K. H. Yao, R. F. Masilamani, M. L. Dustin, A. Rudensky, K. Liu, and M. C. Nussenzweig. 2009. Feedback control of regulatory T cell homeostasis by dendritic cells in vivo. *J. Exp. Med.* 206: 1853–1862.
41. Verginis, P., H. S. Li, and G. Carayanniotis. 2005. Tolerogenic semimature dendritic cells suppress experimental autoimmune thyroiditis by activation of thyroglobulin-specific CD4+CD25+ T cells. *J. Immunol.* 174: 7433–7439.
42. Kretschmer, K., I. Apostolou, D. Hawiger, K. Khazaie, M. C. Nussenzweig, and H. von Boehmer. 2005. Inducing and expanding regulatory T cell populations by foreign antigen. *Nat. Immunol.* 6: 1219–1227.
43. Fukaya, T., H. Takagi, Y. Sato, K. Sato, K. Eizumi, H. Taya, T. Shin, L. Chen, C. Dong, M. Azuma, et al. 2010. Crucial roles of B7-H1 and B7-DC expressed on mesenteric lymph node dendritic cells in the generation of antigen-specific CD4+Foxp3+ regulatory T cells in the establishment of oral tolerance. *Blood* 116: 2266–2276.
44. Movahedi, K., M. Guilliams, J. Van den Bossche, R. Van den Bergh, C. Gysemans, A. Beschin, P. De Baetselier, and J. A. Van Ginderachter. 2008. Identification of discrete tumor-induced myeloid-derived suppressor cell subpopulations with distinct T cell-suppressive activity. *Blood* 111: 4233–4244.
45. Li, Q., P. Y. Pan, P. Gu, D. Xu, and S. H. Chen. 2004. Role of immature myeloid Gr-1+ cells in the development of antitumor immunity. *Cancer Res.* 64: 1130–1139.
46. Almand, B., J. I. Clark, E. Nikitina, J. van Beynen, N. R. English, S. C. Knight, D. P. Carbone, and D. I. Gabrilovich. 2001. Increased production of immature myeloid cells in cancer patients: a mechanism of immunosuppression in cancer. *J. Immunol.* 166: 678–689.
47. Delano, M. J., P. O. Scumpia, J. S. Weinstein, D. Coco, S. Nagaraj, K. M. Kelly-Scumpia, K. A. O'Malley, J. L. Wynn, S. Antonenko, S. Z. Al-Quran, et al. 2007. MyD88-dependent expansion of an immature GR-1(+)CD11b(+) population induces T cell suppression and Th2 polarization in sepsis. *J. Exp. Med.* 204: 1463–1474.
48. Voisin, M. B., D. Buzoni-Gatel, D. Bout, and F. Velge-Roussel. 2004. Both expansion of regulatory GR1+ CD11b+ myeloid cells and anergy of T lymphocytes participate in hyporesponsiveness of the lung-associated immune system during acute toxoplasmosis. *Infect. Immun.* 72: 5487–5492.
49. Goñi, O., P. Alcaide, and M. Fresno. 2002. Immunosuppression during acute *Trypanosoma cruzi* infection: involvement of Ly6G (Gr1(+))CD11b(+)immature myeloid suppressor cells. *Int. Immunol.* 14: 1125–1134.
50. Condamine, T., and D. I. Gabrilovich. 2011. Molecular mechanisms regulating myeloid-derived suppressor cell differentiation and function. *Trends Immunol.* 32: 19–25.
51. Sawanobori, Y., S. Ueha, M. Kurachi, T. Shimaoka, J. E. Talmadge, J. Abe, Y. Shono, M. Kitabatake, K. Kakimi, N. Mukaida, and K. Matsushima. 2008. Chemokine-mediated rapid turnover of myeloid-derived suppressor cells in tumor-bearing mice. *Blood* 111: 5457–5466.
52. Mackay, C. R. 2001. Chemokines: immunology's high impact factors. *Nat. Immunol.* 2: 95–101.
53. Gerard, C., and B. J. Rollins. 2001. Chemokines and disease. *Nat. Immunol.* 2: 108–115.
54. Huang, B., Z. Lei, J. Zhao, W. Gong, J. Liu, Z. Chen, Y. Liu, D. Li, Y. Yuan, G. M. Zhang, and Z. H. Feng. 2007. CCL2/CCR2 pathway mediates recruitment of myeloid suppressor cells to cancers. *Cancer Lett.* 252: 86–92.